PROCEEDINGS OF SCIENCE

Reactor Antineutrino Experiments Double Chooz and RENO

Antoine Collin[*†]
Max-Planck-Institut für Kernphysik, Heidelberg
E-mail: antoine.collin@mpi-hd.mpg.de

The θ_{13} parameter of the PMNS mixing matrix remained unknown until the first hints and estimates by both reactor and beam experiments in 2011. Previously, the most competitive limit set by the Chooz experiment let indeed open the hypothesis of a null value. A precise measurement of a non zero value enables a future observation of the CP violation and the estimate of its phase δ. Three experiments aiming for a precision measurement of the θ_{13} neutrino mixing angle were designed in this context: Double Chooz, RENO and Daya Bay. The latter being the subject of another communication in this same conference, this article will focus on the recent results released by the two former ones. Located at the Chooz nuclear power plant in north-eastern France, Double Chooz is searching for the disappearance of antineutrinos produced by the two reactors. It relies on a two identical detector measurement. The near detector, located at a few hundred meters from the cores, before the impact of θ_{13} is exerted, aims at monitoring the $\overline{\nu}_e$ flux emitted by the reactors. The far detector is located at a distance of about one kilometre from the reactor cores, near the expected first maximum amplitude of the oscillation. The comparison of these two measurements gives an estimate of the deficit induced by the oscillation, cancelling most of systematic uncertainties related to neutrino flux emission and detection. The far detector began data taking in April 2011 and gave the first hint of a non zero value of θ_{13} by a reactor experiment that same year. New analysis enhancements led to the latest results of the experiment, based on a far detector only measurement, published in summer 2014: $\sin^2(2\theta_{13}) = 0.090^{+0.032}_{-0.029}$. Data taking in the near detector is about to start, enabling a significant reduction of both reactor and detector related systematic uncertainties in a near future. The RENO experiment, located near the six Yonggwang reactors in South Korea, is based on the same two detector concept as Double Chooz. The data taking in both detectors began in summer 2011 and the first θ_{13} results were published in 2012. The RENO collaboration released lately in conferences the following results, based on a rate only analysis: $\sin^2(2\theta_{13}) = 0.101 \pm 0.013$. Both results are in agreement with the most precise θ_{13} value of Daya Bay.

XIIth International Conference on Heavy Quarks & Leptons 2014
25-29 August 2014
Schloss Waldthausen, Mainz, Germany

[*]Speaker.
[†]On behalf of the Double Chooz collaboration.

PoS(HQL2014)018

1. Neutrino Mixing and Oscillation

The mixing and oscillations of the three light active neutrinos is a well established phenomenon since its observation in the Super-Kamiokande experiment in 1998 [1], along with deficits formerly observed by solar experiments. In the minimal extension to the Standard Model of particle physics, the U_{PMNS} matrix links the three neutrino flavour states to the mass ones. This matrix is usually expressed as the product of three rotation matrices, corresponding to three different oscillation regimes

$$\begin{pmatrix} \nu_e \\ \nu_\mu \\ \nu_\tau \end{pmatrix} = \begin{pmatrix} 1 & 0 & 0 \\ 0 & c_{23} & s_{23} \\ 0 & -s_{23} & c_{23} \end{pmatrix} \begin{pmatrix} c_{13} & 0 & s_{13}\, e^{-i\delta} \\ 0 & 1 & 0 \\ -s_{13}\, e^{i\delta} & 0 & c_{13} \end{pmatrix} \begin{pmatrix} c_{12} & s_{12} & 0 \\ -s_{12} & c_{12} & 0 \\ 0 & 0 & 1 \end{pmatrix} \begin{pmatrix} \nu_1 \\ \nu_2 \\ \nu_3 \end{pmatrix}, \tag{1.1}$$

where s_{ij} and c_{ij} stand for $\sin\theta_{ij}$ and $\cos\theta_{ij}$ respectively. Thus, four parameters rule the neutrino oscillation: three mixing angles and the CP-violation phase δ.

While the parameters linked to the solar and atmospheric neutrino oscillations have been known through different experiments for over a decade [2], the θ_{13} mixing angle, which can be accessed by accelerator and reactor experiments, remained unmeasured until recently.

2. Reactor Antineutrino Experiments

2.1 Phenomenology and Previous Achievements

Nuclear reactors constitute a pure and intense source of $\overline{\nu}_e$ whose disappearance at a baseline of the kilometre scale is directly related to the θ_{13} mixing angle. Reactor neutrino experiments rely therefore on the measurement of electron flavour disappearance: given the mass-splitting parameters and the energy of the $\overline{\nu}_e$ involved, the two flavour approximation is relevant in these conditions and thus the survival probability writes

$$P(\overline{\nu}_e \to \overline{\nu}_e) \backsimeq 1 - \sin^2(2\theta_{13})\, \sin^2\left(1.27\, \frac{\Delta m^2_{31}\,[\mathrm{eV}^2]\; L\,[\mathrm{m}]}{E\,[\mathrm{MeV}]}\right). \tag{2.1}$$

Held already at the Chooz power plant in the late nineties, the Chooz experiment did not observe any oscillation signal on account of insufficient statistics and too high systematic uncertainties, resulting in an upper limit on the θ_{13} angle [3]. Consequently a new generation of experiments arose in the last decade, aiming for a precision measurement of the θ_{13} parameter through the reduction of both statistic and systematic uncertainties.

2.2 New Generation of Experiments: Precision Experiments

In order to reach a high precision level, current experiments are based on a several site measurement and benefit from innovations in their detector design (see section 2.4). In such a concept, at least one detector is located at a distance of about one kilometre from the reactor cores, near the expected first maximum amplitude of the oscillation effect (see eq. 2.1). In addition, one or more near detectors aim at monitoring the $\overline{\nu}_e$ flux emitted by the reactors and hence are located at a few hundred meters from the cores, before the impact of θ_{13} is exerted. The comparison of these near

and far measurements gives an estimate of the deficit induced by the oscillation, cancelling most of systematic uncertainties related to neutrino flux emission and detection. The sites of the three experiments present very specific features, as the number of reactors and detectors as well as their relative locations. The main characteristics are illustrated in Figure 1.

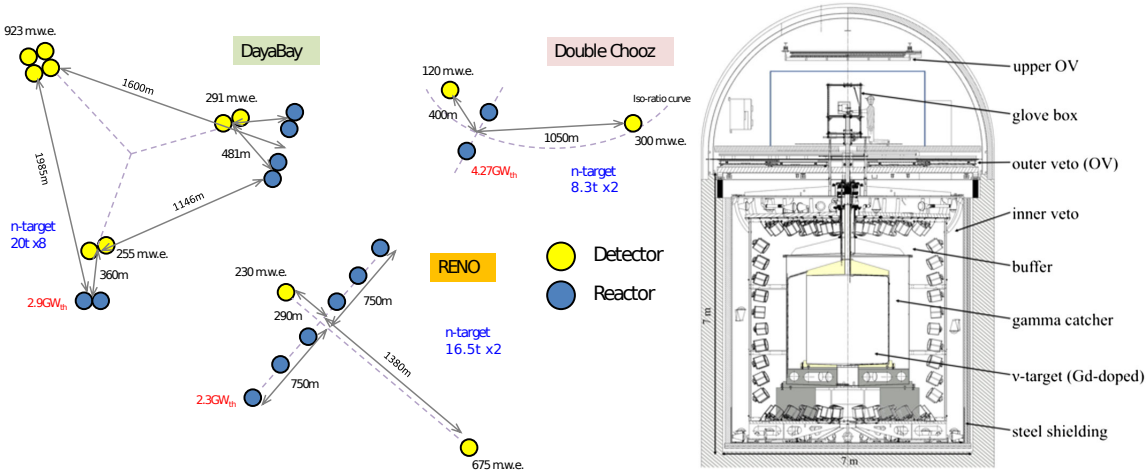

Figure 1: Left: Schematic view of the different experimental sites [4]. Overburden of each detector site is indicated, as well as the thermal power of each individual reactor. **Right:** The Double Chooz far detector [5].

2.3 Antineutrino Detection

The detection of $\overline{\nu}_e$ rely on the inverse β-decay (IBD) in a gadolinium-loaded liquid scintillator, in which a neutrino interacts with a free proton, generating a neutron and a positron: $\overline{\nu}_e + H^+ \rightarrow n + e^+$. The positron is observed as a prompt signal with an energy deposit directly related to the incident neutrino energy: $E_{signal} = E_{\overline{\nu}_e} - 0.8\,\text{MeV}$. The neutron capture, either on Gd or H, constitutes a delayed signal identifying clearly the IBD reaction. The presence of Gd enables to reduce the capture time—from about 200 μs to 30 μs approximately in average—and to shift the signal of the radiative capture above the natural γ radiation background and hence to increase both the efficiency of detection and the signal over background ratio. Indeed Gd captures thermal neutrons with a high cross-section, releasing few γ-rays with a total energy of about 8 MeV.

2.4 Detector Concept

Two parts compose the Double Chooz detectors: the neutrino detector as such, also called Inner Detector (ID), and the vetoes. The ID consists of three cylindrical nested volumes (see Fig. 1). The neutrino target (NT) constitutes the innermost vessel, filled with 10 m^3 of Gd-loaded liquid scintillator. It is surrounded by a 55 cm thick layer of Gd-free liquid scintillator, called the γ-catcher (GC), aiming to retrieve the energy of γ-rays escaping the NT and thus to ensure that the active volume for $\overline{\nu}_e$ detection corresponds exactly to the target. Finally, a 105 cm thick layer of non-scintillating mineral oil, called the buffer, surrounds the two active volumes. The internal boundaries are made of transparent acrylic vessels, whereas the buffer tank, to which 390 low background 10-inch photomultiplier tubes (PMTs) are fixed, is made of stainless steel. The buffer layer provides a shield to radioactive background originating from the PMTs or the surrounding

rock and increases the homogeneity of the light collection as well. The ID itself is surrounded by a 50 cm thick liquid scintillator layer, the Inner Veto (IV), equipped with 78 8-inch PMTs. The IV works not only as an active veto to cosmic ray muons but also as a shield to fast neutrons from outside of the detector. An Outer Veto (OV) of plastic scintillator strips covers the top of the Double Chooz detector providing information on muon hits and enabling muon track reconstruction.

The Daya Bay and RENO detectors are based on the same concept. Main differences reside in smaller buffer layers, 50 cm and 70 cm thick respectively, and in muon veto filled with purified water instead of liquid scintillator. Further information about detector geometries can be found in [5, 6, 7]. This new generation of detectors enabled the first indication of the $\overline{\nu}_e$ disappearance near reactors by Double Chooz [8], followed by the Daya-Bay [6] and RENO [7] results.

2.5 Backgrounds

By reason of their common concept, the three experiments face similar backgrounds, though with different levels. They divide in two groups: the accidental backgrounds and the correlated ones. Random coincidences of two unrelated events—such as a natural γ ray and a neutron capture—constitute the former contribution. The latter one consists of coincidences whose prompt and delayed signals originate from the same physical event. Main correlated backgrounds are composed of three different categories. First the fast neutrons, for which the prompt signal is given by a proton recoil and the delayed one by the radiative capture of the same neutron. Then the stopping muons: the deposited energy along a muon track produces the prompt signal and the Michel electron induced by its decay the delayed one. Finally, β-n decays may ensue from the formation of cosmogenic isotopes through ^{12}C nuclei spallations by muons with a typical constant time in the hundred millisecond range. This is referred to as ^{9}Li–^{8}He background, those isotopes being the two relevant β-n emitters for IBD based detectors. All these contributions have to be estimated in order to be subtracted from the sample of selected IBD candidates.

3. The Double Chooz Analysis and Results

While the Double Chooz far detector is taking data since April 2011, the near detector installation has just been achieved and data taking is consequently about to start on the experiment's near site. Results rely thus on comparison of far detector data with Monte Carlo (MC) simulations.

3.1 Selection of IBD Candidates

The sample of neutrino candidates is selected after the rejection of muons and events occurring within 1 ms after a muon as well as light noise events, induced by light sporadically emitted by some PMT bases. Light noise rejection cuts are based on inhomogeneous charge distribution and signal pulse timing over the ID PMTs. The selection criteria of IBD candidates are defined pursuing a twofold aim: maximizing the efficiency of detection while minimizing the background contribution. The coincidence selection is performed with the following requirements: 1) the energy of the prompt signal satisfies $0.5 < E_{vis} < 20$ MeV; 2) and the delayed energy $4 < E_{vis} < 10$ MeV; 3) the correlation time separating prompt and delayed signals satisfies $0.5 < \Delta T < 150\,\mu$s; 4) and the distance separating them $\Delta R < 1$ m; 5) no event but the delayed one within 200 μs before and 600 μs after the prompt signal (multiplicity cut).

Thanks to wider selection cuts, the detection efficiency has been increased and the corresponding data to MC discrepancy reduced compared to the previous analysis [9]. Indeed, the IBD detection efficiency in MC (with above criteria except for cut 5)) has increased by about 8 %. The trigger efficiency at the prompt energy threshold amounts to about 100 % with negligible uncertainty. Hence, the detection efficiency of the IBD signal and its uncertainty are dominated by the delayed event detection. Two independent analyses using new techniques—one based on neutrons from the ^{252}Cf radioactive source deployed at different locations in the NT and the other one on neutrons induced by IBD reactions—led to a factor two reduction of the detection systematic uncertainty compared to the last publication.

3.2 Background Estimation

Despite the optimization of selection criteria towards background contamination, some background events pass the cuts (see section 2.5) and should be carefully studied and subtracted from the candidates' sample. New vetoes have been introduced in this analysis, they are applied along with the selection cuts defined above and enable a significant improvement of signal over background ratio. The prompt candidates in coincidence with an OV trigger are rejected. Furthermore, if a prompt event and an energy deposition in IV occur within 50 ns, the IBD candidate is rejected as well. In order to reduce rejection of accidental coincidences, the distance separating the prompt candidate and the IV event is required to be less than 3.7 m.

The likelihood output value F_V of the vertex reconstruction algorithm (see [5] for further details) enables to quantify the delayed event dissimilarity from a point-like source. The stopping muons enter the detector through the chimney. Therefore, their PMT hit pattern differ from other physics events, and a veto based on the F_V value provides a high rejection of their contribution.

A likelihood test, based on the distance to parent muon track and on the number of generated neutrons, enables to veto a large part of ^{9}Li+^{8}He events. The Figure 2 (left) depicts the impact of the different vetoes. After 12 MeV, no neutrino signal is expected; in this energy region of the prompt spectrum, the vetoes reject about 90 % of IBD candidates.

Background	Rate (d^{-1})	Gd-III/Gd-II
^{9}Li+^{8}He	$0.97^{+0.41}_{-0.16}$	0.78
Fast-n + stopping μ	0.604 ± 0.051	0.52
Accidentals	0.070 ± 0.003	0.27
^{13}C(α,n)^{16}O reactions	< 0.1	not reported in Gd-II
^{12}B	< 0.03	not reported in Gd-II

Table 1: Summary of background rate estimates. Gd-III/Gd-II represents the reduction of background rates with respect to the previous DC publication [9], after scaling to account for different selection criteria.

The accidental background rate and energy spectrum can be measured very accurately by looking for coincidences with several shifted time windows. The remaining ^{9}Li+^{8}He contribution is studied by searching for coincidences with a muon event. The likelihood test enables also to select a ^{9}Li+^{8}He sample, providing the spectral shape. To extract fast neutrons and stopping μ contamination, coincidences with energy deposition in IV are used. Other background contributions were studied and have proven to be negligible. The Table 1 gives the background rate estimates.

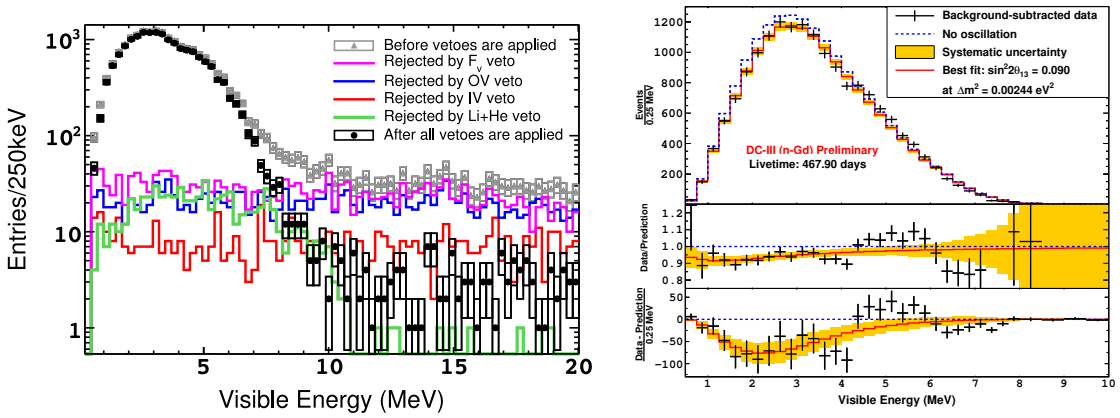

Figure 2: Left: Prompt energy spectrum before (gray) and after all vetoes are applied. The events rejected by each individual veto are represented in color lines. **Right:** Energy spectrum of IBD candidates after background subtraction (black) along with predictions with no oscillation (blue) and for the R+S best fit (red). The bottom panels show the ratio as well as the deficit of data compared to predictions [5].

3.3 Neutrino Oscillation Analysis

In the 460.67 live day period on which the analysis is based, 17,351 IBD candidates—including backgrounds detailed above—are observed during reactor-on phase while $18{,}290^{+370}_{-330}$ where expected in absence of neutrino oscillation. Double Chooz also collected 7.24 days of data with both reactors off [10]. The predicted number of IBD candidates, including residual $\overline{\nu}_e$ contribution, amounts to $12.9^{+3.1}_{-1.4}$ whereas 7 were observed. The compatibility of both numbers is 9 % (1.7 σ). The reactor-off measurement is used not only to cross-check the background estimates but also to constraint the total background rate in the oscillation analysis.

	Uncertainty	Gd-III/Gd-II
Reactor flux	1.7 %	1
Detection efficiency	0.6 %	0.6
^{9}Li+^{8}He background	+1.1 / – 0.4 %	0.5
Fast-n and stopping muon BG	0.1 %	0.2
Statistics	0.8 %	0.7
Total	+2.3 / – 2.0 %	0.8

Table 2: Signal and background uncertainties relative to the signal prediction. The last column gives the reduction factor compared to previous publication [9].

The deficit of observed candidates is interpreted as a consequence of the neutrino oscillation in a two flavour framework (see Eq. 2.1) and θ_{13} is extracted by a χ^2 fit taking also advantage of the spectral shape information, therefore referred to as *Rate+Shape* (R+S). Normalization uncertainties are summarized in Table 2. The prompt energy spectrum is divided in bins of variable sizes (see Figure 2, right), background rates and shapes originating from studies described above (section 2.5) are used. Covariance matrices account for the statistical and systematic uncertainties, including bin-to-bin correlations. Additional pull terms take into account other possible systematic effects affecting the neutrino prediction such as energy scale, correlated background rates and

the value of Δm^2_{31}. The best fit value is obtained at $\sin^2(2\theta_{13}) = 0.090^{+0.032}_{-0.029}$ (stat.+ syst.) with χ^2_{min}/NDF = 52.2/40. The corresponding fit output value of background rates is 1.38 ± 0.14 events per day, consistent with estimates of Table 1. Additional information provided by the spectral shape enables to reduce the uncertainty.

While the oscillation framework accounts for deficit of detected events compared to expectations at low energy (Figure 2 right, lower panels), discrepancies are observed above 4 MeV. The distortion is characterized by an excess of events up to 6 MeV and a deficit above. Owing to the value of Δm^2_{31}, the impact of oscillations is limited at lower energies and this spectral distortion does not affect the θ_{13} measurement. Cross-checks showed that the excess between 4.25 and 6 MeV is correlated to the reactor power, disfavouring thus the hypothesis of unknown background as origin.

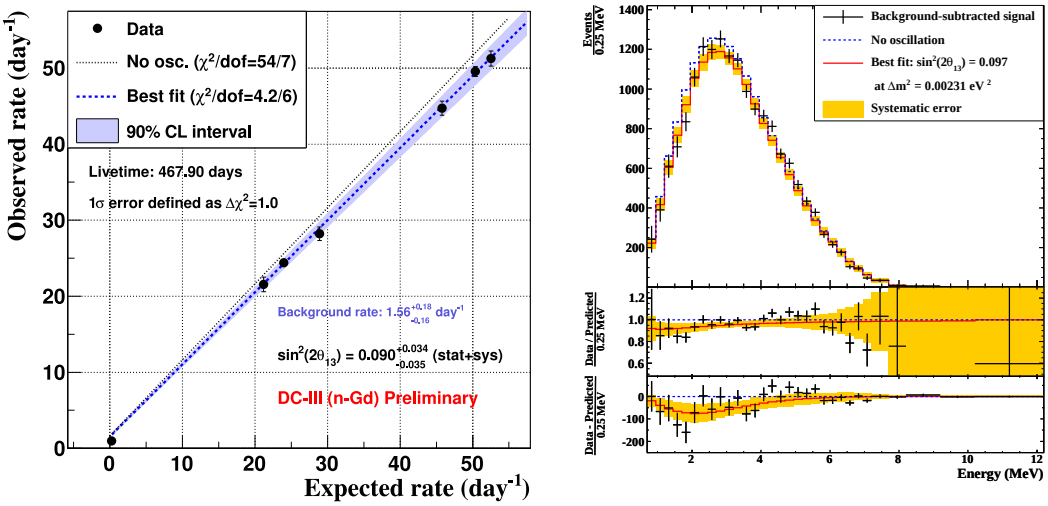

Figure 3: Left: Correlation between the measured daily candidate rate and the expected neutrino rate. The blue line corresponds to the best RRM fit. **Right:** Energy spectrum of nH $\overline{\nu}_e$ candidates and best fit [11].

Another fit framework takes advantage of the variation of the number of detected candidates according to the expectations, which are a function of the reactors' power. This analysis is therefore called *Reactor Rate Modulation* (RRM). Data are divided in seven bins according to the reactor power conditions: from two reactors off up to two reactors at full power. Considering the number of detected candidates as a function of expected ones, θ_{13} can be fitted as the slope while the daily background rate B constitutes the intercept (see Figure 3 left). With the constraint on B coming from background studies (see Table 1), the RRM fit results in $\sin^2(2\theta_{13}) = 0.090^{+0.034}_{-0.035}$ and $B = 1.56^{+0.18}_{-0.16}$, both in good agreement with R+S fit and background estimates respectively.

Instead of the radiative capture of neutrons on Gd nuclei, the capture on H, releasing a 2.2 MeV γ-ray, can be used as delayed IBD signal. This enables to increase the statistics of candidates, both the NT and GC working as detection volumes. On the other hand, the accidental background is substantially increased because of the higher natural γ-ray background around 2 MeV. The ensuing reduction of the signal over background ratio leads consequently to larger systematic uncertainties. Selection cuts are adjusted to the features of H captures, especially with respect to correlation time and delayed energy windows. Further details about the $\overline{\nu}_e$ candidates' selection and systematic

uncertainty studies can be found in [11]. A Rate+Shape fit is carried out, with similar principles as the Gd Analysis one, leading to the following estimation: $\sin^2(2\theta_{13}) = 0.097 \pm 0.048$ (stat.+ syst.). The Figure 3 (right panel) shows the background subtracted energy spectrum of IBD candidates and the comparison to predictions and fit output.

4. The RENO Results

The definition of the IBD candidate selection criteria follows the same principles as for Double Chooz. It leads to slightly different cuts, more details can be found in [12]. The RENO experiment faces the same backgrounds than Double Chooz, though with different amounts because of different overburden, shielding, selection cuts and accidental contamination. Owing to an incident with the calibration source container, a small fraction of ^{252}Cf has contaminated the liquid scintillator since fall 2012. This contamination adds a background contribution to be taken into account in the RENO analysis. Background rate estimates are summarized in Table 3.

	Rate (d^{-1})	
Background	Near	Far
^{9}Li+^{8}He	8.28 ± 0.66	1.85 ± 0.20
Fast-n + stopping μ	2.09 ± 0.06	0.44 ± 0.02
Accidentals	1.82 ± 0.11	0.36 ± 0.01
^{252}Cf	0.28 ± 0.05	1.98 ± 0.27

Table 3: Summary of background rate estimates in the RENO near and far detectors [13].

Life time, number of IBD candidates as well as estimated background events are given in Figure 4, along with the prompt energy spectrum of candidates. A Rate only fit, based on the deficit of observed candidates integrated over the whole energy spectrum, is then performed, resulting in the following estimation: $\sin^2(2\theta_{13}) = 0.101 \pm 0.013$ (stat.+ syst.) [13].

Although a R+S fit, taking advantage of the spectral information, has not been released yet, the RENO collaboration reported progress status of their command over the energy scale [13]. The collaboration is working on this issue and update is expected soon on this matter.

The RENO collaboration also reported an excess of detected events between 4 and 6 MeV both in its near and far detectors (see Figure 4 right). This excess has proven to be correlated with the total reactor power, which strongly disfavours any additional background contribution.

The RENO collaboration performed an IBD candidate selection with neutron capture on H as well. In a Rate only fit framework, this analysis leads to the following estimation of the θ_{13} mixing angle: $\sin^2(2\theta_{13}) = 0.095 \pm 0.030$ (stat.+ syst.) [13].

5. Current Achievements and Future Sensitivities

After first hints for a non zero value of θ_{13} given by accelerator experiments [14], the new generation of reactor experiment enabled to observe the first indication of the $\overline{\nu}_e$'s disappearance close to reactors, observation reported by Double Chooz in 2011. This indication was followed the

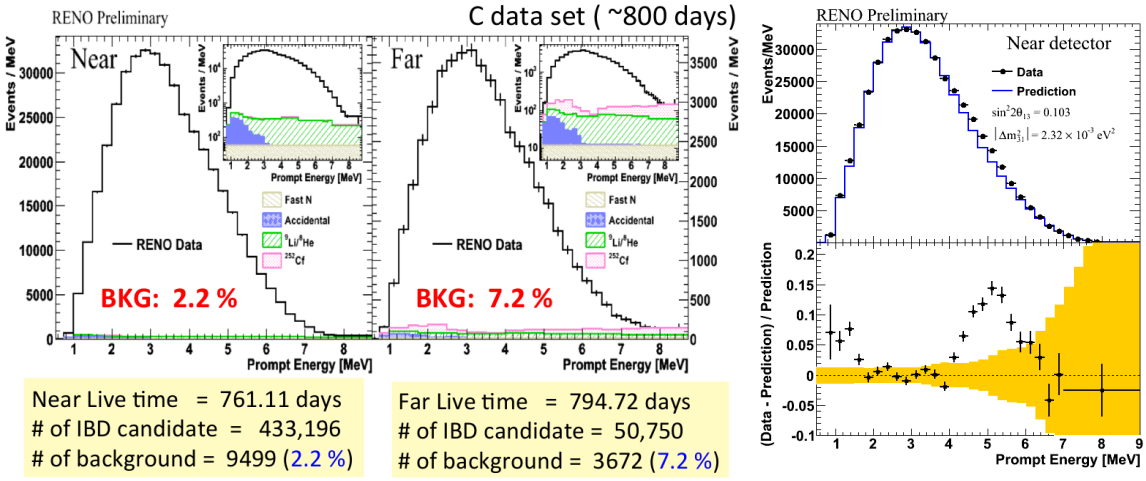

Figure 4: Prompt energy spectra in near and far detectors with estimated background contributions (left) [13] and compared to the prediction of IDB candidates in the near detector (right) [15].

next year by the first precision measurements of θ_{13} by Daya Bay and RENO. Since then, measurements of the three experiments have improved, not only because of increasing statistics, but also owing to analysis enhancements. All estimates of θ_{13} published so far are consistent. Complementary analyses, using for instance IBD neutron capture on H, resulted in valuable cross-checks. The current most precise measurement of Double Chooz amounts to $\sin^2(2\theta_{13}) = 0.090^{+0.032}_{-0.029}$ [5]. The RENO collaboration, running with two detectors, released recently in conferences the following result based on a rate only analysis: $\sin^2(2\theta_{13}) = 0.101 \pm 0.013$ [13].

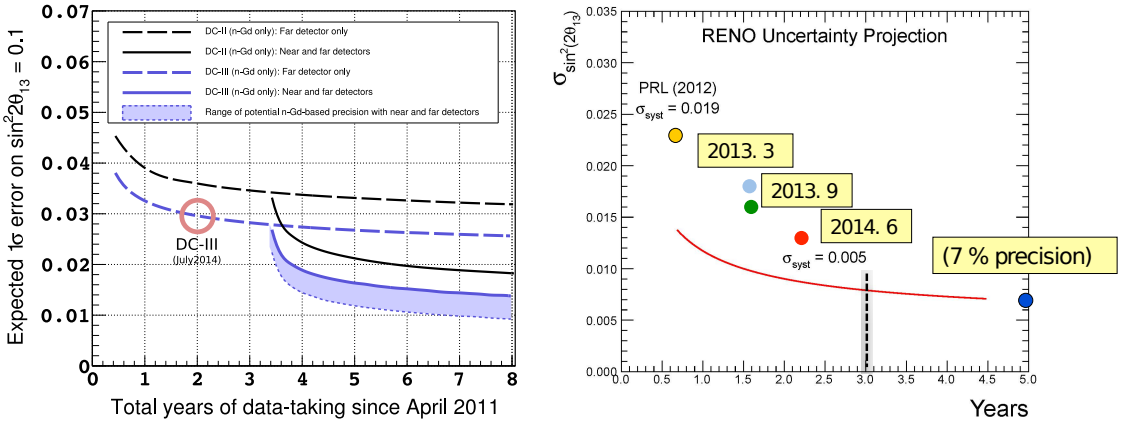

Figure 5: Future sensitivities of the Double Chooz (left) and RENO [13] (right) experiments.

The impending phase of data taking with two detectors will result in a significant improvement of the Double Chooz sensitivity, owing to a substantial decrease of systematic uncertainties originating in the relative two detector comparison. Indeed, the uncertainty coming from the reactor flux prediction—currently the dominating one—as well as correlated uncertainties will cancel. The Figure 5 (left) shows the projected sensitivities of a Gd-based analysis under different assump-

tions. Sensitivities are given with respect to previous publication (black) and current one (blue) analysis techniques, illustrating the improvements recently brought. Dashed lines represent far detector only analyses, while solid ones show sensitivities for two detector measurements, for which a 0.1 % uncertainty on the reactor flux and 0.2 % uncertainty on the detection efficiency and backgrounds are assumed. The shaded area depicts the reachable sensitivity region with further analysis improvements, the lower limit corresponding to sensitivity without any systematic uncertainty but the reactor one.

The Figure 5 (right) depicts the precision of RENO results published so far as well as projected sensitivity in the future. Significant further improvements of the systematic uncertainty are expected, enabling to reach a 7 % precision measurement within the next two years.

References

[1] Y. FUKUDA, et al., *Evidence for oscillation of atmospheric neutrinos*, Phys. Rev. Lett. 81, pp. 1562–1567 (1998).

[2] J. BERINGER, et al. (Particle Data Group), Phys. Rev. D86, p. 010001 (2012) and 2013 partial update for the 2014 edition.

[3] M. APOLLONIO, et al., *Search for neutrino oscillations on a long baseline at the Chooz nuclear power station*, Eur. Phys. J, C27, pp. 331–374 (2003).

[4] T. KONNO, *Measurement of θ_{13} by neutrino oscillation experiments*, talk at the 47^{th} Rencontres de Moriond on Cosmology (2012).

[5] Y. ABE, et al., *Improved measurements of the neutrino mixing angle θ_{13} with the Double Chooz detector*, JHEP 10 (2014) 086, arXiv:1406.7763 [hep-ex].

[6] F.P. AN, *Observation of electron-antineutrino disappearance at Daya Bay*, Phys. Rev. Lett. 108, p. 171803 (2012).

[7] J.K. AHN, et al., *Observation of reactor electron antineutrino disappearance in the RENO experiment*, Phys. Rev. Lett. 108, p. 191802 (2012).

[8] Y. ABE, et al., *Indication for the disappearance of reactor electron antineutrinos in the Double Chooz experiment*, Phys. Rev. Lett. 108, p. 131801 (2012).

[9] Y. ABE, et al., *Reactor electron antineutrino disappearance in the Double Chooz experiment*, Phys. Rev. D86, p. 052008 (2012).

[10] Y. ABE, et al., *Direct Measurement of Backgrounds using Reactor-Off Data in Double Chooz*, Phys. Rev. D87, p. 011102 (2013).

[11] Y. ABE, et al., *First Measurement of θ_{13} from Delayed Neutron Capture on Hydrogen in the Double Chooz Experiment*, Phys. Lett. B723, pp. 66-70 (2013).

[12] S.-H. SEO, *New Results from RENO*, Proceedings of XVth International Workshop on Neutrino Telescopes, Venice, Italy (2013).

[13] S.-H. SEO, *New Results from RENO*, talk at the XXVI International Conference on Neutrino Physics and Astrophysics, Boston (2014).

[14] K. ABE, et al., *Indication of Electron Neutrino Appearance from an Accelerator-produced Off-axis Muon Neutrino Beam*, Phys. Rev. Lett. 107, p. 041801 (2011).

[15] Courtesy of Prof. S.-B. Kim, Seoul National University, spokesperson of the RENO collaboration.